Science of the Total Environment 595 (2017) 149–158

Contents lists available at ScienceDirect

Science of the Total Environment

journal homepage: www.elsevier.com/locate/scitotenv

Airborne measurements of isoprene and monoterpene emissions from southeastern U.S. forests

Haofei Yu [a,b], Alex Guenther [b,c,*], Dasa Gu [b,c], Carsten Warneke [d,e], Chris Geron [f], Allen Goldstein [g], Martin Graus [h], Thomas Karl [h], Lisa Kaser [i], Pawel Misztal [g], Bin Yuan [d,e]

[a] Dept. of Civil, Environmental & Construction Engineering, University of Central Florida, Orlando, FL, USA
[b] Pacific Northwest National Laboratory, Richland, WA 99354, USA
[c] Department of Earth System Science, 3200 Croul Hall, University of California, Irvine, CA 92697-3100, USA
[d] Chemical Sciences Division, Earth System Research Laboratory, NOAA, Boulder, CO, USA
[e] CIRES, University of Colorado, Boulder, CO, USA
[f] National Risk Management Research Laboratory, U.S. Environment Protection Agency, Raleigh, NC, USA
[g] Department of Environmental Science, Policy, and Management, University of California, Berkeley, CA, USA
[h] Institute of Atmospheric and Cryospheric Sciences, University of Innsbruck, Innsbruck, Austria
[i] National Center for Atmospheric Research, Boulder, CO, USA

HIGHLIGHTS

- Aircraft eddy covariance and inverse modeling BVOC flux measurements agree.
- Models should account for differing emission factors in upper and lower canopy.
- Modeled and measured emissions agree for landscapes with high emitters.

GRAPHICAL ABSTRACT

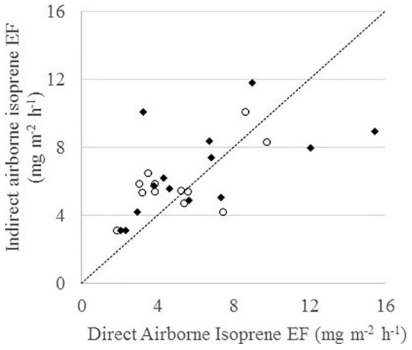

ARTICLE INFO

Article history:
Received 5 January 2017
Received in revised form 28 March 2017
Accepted 28 March 2017
Available online xxxx

Editor: D. Barcelo

Keywords:
Isoprene
Monoterpenes
Biogenic volatile organic compounds
Aircraft flux measurements
Model of Emissions of Gases and Aerosols from Nature (MEGAN)

ABSTRACT

Isoprene and monoterpene emission rates are essential inputs for atmospheric chemistry models that simulate atmospheric oxidant and particle distributions. Process studies of the biochemical and physiological mechanisms controlling these emissions are advancing our understanding and the accuracy of model predictions but efforts to quantify regional emissions have been limited by a lack of constraints on regional distributions of ecosystem emission capacities. We used an airborne wavelet-based eddy covariance measurement technique to characterize isoprene and monoterpene fluxes with high spatial resolution during the 2013 SAS (Southeast Atmosphere Study) in the southeastern United States. The fluxes measured by direct eddy covariance were comparable to emissions independently estimated using an indirect inverse modeling approach. Isoprene emission factors based on the aircraft wavelet flux estimates for high isoprene chemotypes (e.g., oaks) were similar to the MEGAN2.1 biogenic emission model estimates for landscapes dominated by oaks. Aircraft flux measurement estimates for landscapes with fewer isoprene emitting trees (e.g., pine plantations), were about a factor of two lower than MEGAN2.1 model estimates. The tendency for high isoprene emitters in these landscapes to occur in the shaded understory, where light dependent isoprene emissions are diminished, may explain the lower than expected emissions. This result demonstrates the importance of accurately representing the vertical profile

* Corresponding author at: University of California, Irvine, CA 92697, USA.
E-mail address: alex.guenther@uci.edu (A. Guenther).

http://dx.doi.org/10.1016/j.scitotenv.2017.03.262
0048-9697/

of isoprene emitting biomass in biogenic emission models. Airborne measurement-based emission factors for high monoterpene chemotypes agreed with MEGAN2.1 in landscapes dominated by pine (high monoterpene chemotype) trees but were more than a factor of three higher than model estimates for landscapes dominated by oak (relatively low monoterpene emitting) trees. This results suggests that unaccounted processes, such as floral emissions or light dependent monoterpene emissions, or vegetation other than high monoterpene emitting trees may be an important source of monoterpene emissions in those landscapes and should be identified and included in biogenic emission models.

1. Introduction

It is widely recognized that terrestrial ecosystems produce and emit a large variety of biogenic volatile organic compounds (BVOCs) into the atmosphere and this flux dominates the global budget of VOC emissions from all sources combined (Guenther et al., 1995; Kesselmeier and Staudt, 1999; Goldstein and Galbally, 2007; Lamarque et al., 2010). Most BVOC, including isoprene and monoterpenes, are highly reactive and have significant roles in both daytime and nighttime atmospheric chemistry (Zhang et al., 2000; Brown et al., 2009). This includes their contribution to the formation of Secondary Organic Aerosol (SOA) (Carlton et al., 2009), which is a major air quality issue and a significant uncertainty in climate change simulations (Pachauri et al., 2014). Furthermore, BVOC are an important precursor to ground level ozone in rural and populated urban areas (Chameides et al., 1988; Guo et al., 2012). As one of the six Criteria Air Pollutants regulated under the National Ambient Air Quality Standards, ground level ozone poses substantial threats to human health and public welfare in the U.S. (U.S. Environmental Protection Agency, 2014).

To quantify the impact of isoprene and monoterpenes on climate and air quality, accurate prediction of the spatiotemporal distributions of emissions is needed. Numerical approaches, including the Model of Emissions of Gases and Aerosols from Nature (MEGAN, Guenther et al., 2006, 2012), are dependent on the availability of accurate landcover distributions including the foliage area per unit ground area (Leaf Area Index, LAI, $m^2\ m^{-2}$) of vegetation covered surfaces, which we refer to as LAIv, and the relative composition of different plant chemotypes, which are plant species with differing capacities to emit BVOCs. MEGAN BVOC emissions are driven by global LAIv and chemotype fractions data that are estimated using satellite based landcover distributions calibrated using ground based vegetation measurements. This may require high resolution, regional specific information to supplement global datasets in heterogeneous landscapes such as urban areas (Kota et al., 2015). In addition to the need for distributions of chemotypes, it is necessary to specify the emission factors associated with each chemotype. The lack of direct measurements has made it difficult to evaluate the isoprene emission factors (EFs) used in regional to global emissions models (Warneke et al., 2010; Zare et al., 2012). These EF databases have primarily been based on measurements from enclosure experiments at leaf or branch level and have been evaluated by comparison to boundary layer concentrations and tower based eddy flux measurements (Guenther et al., 2006). Evaluations of isoprene EF databases in the eastern US have reported differences of about a factor of two between observed and predicted isoprene concentrations and note that this is within the uncertainty of the indirect measurement approach (Carlton and Baker, 2011; Kota et al., 2015; Warneke et al., 2010). A recent study by Kota et al., 2015; compared the global MEGAN BVOC emission model with tower eddy flux measurements in an urban area and concluded that the EF were too high and the LAI values were too low demonstrating the need for better inputs in heterogeneous areas such as urban landscapes. The eddy covariance flux measurement approach, which provides a direct measurement of isoprene emissions and largely simplifies the interpretation of chemical losses and boundary layer dynamics, has recently been extended from canopy to regional scales using airborne eddy flux measurement techniques (Karl et al., 2009). Previous applications of this technique have quantified the VOC emissions of individual shale gas facilities in the southeastern US (Yuan et al., 2015) and have demonstrated that the MEGAN model can accurately simulate isoprene EF distributions across oak woodlands and other landscapes in California (Misztal et al., 2014, 2016).

In this study, we derive high resolution isoprene and monoterpene flux estimates from aircraft eddy covariance observations collected in the southern US during the 2013 SAS (Southeast Atmosphere Study) and compare direct and indirect flux measurement approaches. We assess the landcover and environmental data available for relating emission rates to emission factors and consider the uncertainties involved in both. The emission factors calculated for high emission chemotypes are described and compared with the values used for MEGAN and the implications for regional BVOC emission modeling are discussed.

2. Methods

2.1. Landcover and meteorological data

2.1.1. LAI foliar distributions

LAI refers to projected one-sided green leaf area per unit ground surface area (m^2 of leaf area / m^2 of ground area). The LAI of vegetation covered surfaces, LAIv, is defined as

$$\mathrm{LAIv} = \mathrm{LAI}/\mathrm{f_c} \quad (1)$$

where f_c is the area fraction that is covered by living vegetation. For this study, 8 day averaged LAI data for North America were retrieved from the MODIS (MOderate Resolution Imaging Spectroradiometer) satellite product Collection 5 (MCD15A2) (Fang et al., 2013) for the study period and combined with climatological maximum green vegetation fraction data (Broxton et al., 2014) based on MODIS remote sensing products MCD12Q1 and MOD13A2. Spatial resolution of the LAIv data is approximately 900 m and the temporal resolution is 8 days. A multiyear LAIv database (years 2003 to 2013) was compiled to investigate the importance of using LAIv for the specific campaign period.

2.1.2. Vegetation type distributions

Vegetation species have vastly different capabilities to produce and emit BVOC and thus information on the distributions of the abundance of high and low emitting plant species is needed for realistic regional BVOC emission estimates (Rasmussen, 1970). The MEGAN2.1 model adopted the 16 CLM (Community Land Model) Plant Functional Type (PFT) schemes (Oleson et al., 2013) as the first step in categorizing spatial variations in BVOC emission chemotypes. PFTs are broad categories of vegetation (e.g. temperate broadleaf deciduous trees and boreal evergreen shrubs) with average emission factors that differ substantially. Emission capacities of different plant species within a PFT can still vary considerably. For this project, the global PFT database described by Guenther et al. (2012) was updated to produce a 30 m resolution PFT database, following the CLM4.5 PFT scheme, for the contiguous US.

The CLM 16 PFT scheme was designed to represent variability in land-surface exchange processes, including water and energy fluxes, but it does not fully capture BVOC emission variations. For example,

both oak (*Quercus* sp.) trees and maple (*Acer* sp.) trees are classified as broadleaf deciduous temperate tree PFT but oak trees are high isoprene emitters while maples have negligible isoprene emissions. In order to capture such differences, each PFT must be divided into chemotypes with representative BVOC emission capacities. The chemotype distribution dataset described by Guenther et al. (2012) was updated for this study using the high resolution (30-m) LANDFIRE existing vegetation type (EVT) database (Ryan and Opperman, 2013) in place of the relatively broad ecoregion scheme described by Omernik and Griffith (2004). As an example of the difference between the two schemes, an extensive region of the mid-elevation, eastern slope of the southern Rocky Mountains is classified by the ecoregion schemes as "21c: Crystalline mid-elevation forests" dominated by a mixture of aspen, ponderosa pine, Douglas-fir, lodgepole pine and limber pine. While the average tree species composition for this ecoregion is reasonable, specific locations can differ considerably and are better represented by the LANDFIRE scheme which includes a mosaic of nearly monodominant stands of aspen (LANDFIRE EVT 3011: Rocky Mountain Aspen Forest and Woodlands) and ponderosa pine (LANDFIRE EVT 3054: Southern Rocky Mountain Ponderosa Pine Woodland) along with several mixed forest categories.

2.1.3. Meteorological data

BVOC emissions are highly sensitive to canopy temperature and solar radiation and comparisons of aircraft flux measurements with emission models are dependent on the accuracy of the meteorological driving variables used to relate emissions to emission factors. Two meteorological (temperature and solar radiation) datasets were used for this study. One dataset consisted of meteorological fields extracted from the North American Land Data Assimilation System (NLDAS-2) forcing data (Xia et al., 2012) and the second dataset was based on output from a Weather and Research Forecasting (WRF) model simulation conducted for the study period.

2.2. Aircraft flux measurements

2.2.1. Airborne eddy covariance

The wavelet based Airborne Eddy Covariance (AEC) method is a powerful mathematical tool for the analysis of trace gas fluxes from airborne measurement data (Mauder et al., 2007; Karl et al., 2009; Karl et al., 2013; Misztal et al., 2014, 2016). Compared with the traditional eddy-covariance method that is based on Fast Fourier Transform (FFT), the AEC method relaxes the stationarity requirement and enables investigation of flux contributions from temporally varying spectra resulting in flux estimates with higher spatial resolution. These highly resolved measurements are useful for areas with relatively heterogeneous surface topography or landcover, such as in the southeastern US. In a previous study (Karl et al., 2013; Misztal et al., 2014, 2016), high resolution flux data were derived using the AEC method, together with vertical flux divergence corrections, were successfully applied to investigate regional isoprene emissions from California landscapes including oak woodlands. In this study, we applied this method to fast response isoprene and total monoterpene data collected with a PTR-MS (Proton Transfer Reaction - Mass Spectrometry) instrument on-board the NSF/NCAR C-130 aircraft for the Nitrogen, Oxidants, Mercury and Aerosol Distributions, Sources and Sinks (NOMADSS) component of the SAS campaign, during 19 research flights conducted in summertime between June 1 and July 15, 2013. The NOMADSS PTR-MS and other C130 measurements are described by Kaser et al. (2015).

Horizontal flight periods selected for flux analysis, referred to as flux legs here, excluded sudden aircraft movements such as substantial changes in roll, pitch and yaw angles. About 70% of the flux measurements are associated with flight patterns, referred to here as "racetracks", consisting of oval shaped patterns at multiple vertical heights enabling direct determination of planetary boundary layer (PBL) heights from vertical profiles of isoprene concentration, potential temperature, virtual potential temperature, water vapor mixing ratio and horizontal wind speed. The racetrack flight patterns also provided a large number of replicate measurements at multiple horizontal locations within a landscape. The isoprene vertical flux profiles were also used to characterize the flux divergence between the top of the canopy and the height of the aircraft measurement. The remaining flux measurements were made at additional locations at a single altitude within the PBL and are referred to as "transect" measurements here.

Delay time between BVOC concentration measured by the PTR-MS instrument and the aircraft turbulence measurements were determined by examining covariance between vertical wind and isoprene concentrations. Flux legs were rejected if the estimated delay times were outside of expected values or if there was no clear peak in covariance.

For quality assurance purposes, systematic error, random error and disjunct errors (Lenschow et al., 1994; Karl et al., 2013) were calculated for each flux leg. Flux legs with significantly higher errors, mostly short flight legs, were rejected in later analysis. Additional quality assurance measures were also performed. First, for each flux leg, concentrations and fluxes were calculated using the traditional FFT approach and compared with the mean wavelet flux. Cross-spectra of the two methods were also calculated and compared. Flux legs that did not have similar values for the two methods were rejected and were not used in further analyses.

Estimating the flux at the top of the canopy requires estimates of two factors: 1) the measured flux at the altitude at which the aircraft was flying and 2) the vertical flux divergence which is the rate of change in flux per change in altitude. To estimate the vertical flux divergence, we first obtained vertical profiles of isoprene flux by averaging the estimated isoprene flux from measurements at different altitude levels where the aircraft flew in a stacked racetrack pattern. We then normalized the profile using PBL height to reduce the impact of changing PBL height over time. Isoprene fluxes at the top of the canopy were then calculated using a vertical flux divergence correction method (Misztal et al., 2014) that assumes a linear relationship between fluxes at different altitudes. In addition, although the wavelet based approach provides high resolution flux data, there are considerable uncertainties for individual fluxes at such high resolution. We therefore spatially averaged the extrapolated surface fluxes to 2 km resolution and performed subsequent analysis based on the spatially averaged data. The 2 km spatial resolution still provides exceptional information for characterizing emissions in heterogeneous landscapes and is a major improvement over traditional aircraft flux estimation approaches with spatial resolution of 40 km or more.

2.2.2. Airborne inverse model emission estimate

Isoprene fluxes were also derived using an inverse model technique which has been a traditional approach for estimating isoprene emissions in highly diverse landscapes such as tropical rainforests (Zimmerman et al., 1988) and other landscapes including in the southeastern U.S. (Greenberg et al., 1999). This approach assumes that isoprene concentrations, sources and sinks are at approximately steady state conditions so that the mass of isoprene in the vertical column above a surface is equal to the product of the isoprene lifetime and the difference between the surface emission rate and the entrainment rate at the top of the boundary layer. It is typically assumed that isoprene is relatively well mixed in the daytime mixed layer, and is nearly absent above the boundary layer, so that the vertical column integrated mass of isoprene can be estimated from the concentration measured at a single height within the mixed layer. Guenther et al. (1996) discuss the uncertainties associated with this approach and note that the total uncertainty is dominated by estimates of isoprene lifetime which is dominated by the uncertainty in OH concentration.

The inverse model flux estimates for this study were calculated using the procedures described by Warneke et al. (2010). Fluxes were estimated from airborne PTRMS isoprene measurements on the NCAR C130, and on the NOAA P-3 aircraft deployed for the SENEX component

(Warneke et al., 2016) of the SAS study. The OH concentration estimates used for the calculations were within the range of values determined by two independent observational approaches, in-situ Chemical Ionization Mass Spectrometer and isoprene vertical flux divergence, aboard the NCAR C130 (Kaser et al., 2015). As discussed in more detail by Karl et al. (2013), the isoprene vertical flux divergence (the decrease in isoprene flux with increasing altitude) is determined by the isoprene loss rate which is primarily driven by OH concentrations and so there is a direct relationship between isoprene vertical flux divergence and the concentration of OH.

2.2.3. Flux footprint estimation

The landcover heterogeneity present in many landscapes requires an accurate characterization of the exact footprint of each aircraft flux measurement in order to relate the measured flux to the representative surface landcover characteristics and micrometeorological conditions. An example of a series of aircraft isoprene flux measurement footprints in relation to the heterogeneity in the abundance of isoprene emitting trees in a southeastern U.S. landscape is shown in Fig. 1. For this study, we further refined the footprint analysis method used by Misztal et al. (2014) and performed a detailed half-dome footprint analysis. As illustrated in Fig. 1, the size and directions of half-domes vary spatially and there is substantial spatial heterogeneity of isoprene emitting species within adjacent footprints.

The radius of the half-dome footprint estimated for eddy covariance fluxes was calculated as:

$$dx_{0.5} = 0.9\left[\left(u\, {z_m}^{2/3}\, h^{1/3}\right)/w^*\right] \quad (2)$$

where $dx_{0.5}$ is the half-width of the horizontal footprint (radius); u is horizontal wind speed, extracted from high resolution C-130 aircraft data; z_m is aircraft height above ground, calculated from C-130 aircraft GPS mean sea level altitude and high resolution ground elevation data; h is PBL height taken from C-130 aircraft vertical profiles. If no vertical profiles were available, h was extracted from WRF data provided by the HiRes2 air quality forecasting system (https://forecast.ce.gatech.edu/hires_about.php; Odman et al., 2007; Hu et al., 2010); w^* is convective velocity scale, derived from C-130 aircraft latent heat flux measurements, which was also calculated based on the wavelet approach. The upwind direction to which the half-dome is facing was calculated from the C-130 aircraft horizontal wind direction data. Vector decompositions were performed to obtain spatially averaged wind speed and wind directions. The estimated half-domes were used to determine the extent of the footprint for each aggregate measurement and to define the corresponding area over which to average the 30 m landcover data.

Averaging continuous variables, such as PFT fraction, within a footprint is a straightforward process but determining the average of discrete data, such as the LANDFIRE EVT landcover types, is more challenging. The simplest approach is to determine the dominant EVT, the landcover type that occurs most frequently, within a footprint and assign that dominant EVT to the entire footprint. This approach is easy to implement but does not account for the presence of some high isoprene emission landcover types within a landscape dominated by a low emission EVT, or low isoprene landcover in a landscape dominated by a high emission EVT. As a result, an EVT with no isoprene emitters can be associated with substantial measured isoprene due to the presence of some high emitting EVT in the landscape. To account for this, we used Forest Inventory and Analysis (FIA version 1.0, Miles et al., 2001) species composition data for each EVT to estimate the expected emission contributions of the non-dominant EVTs and used this to adjust the emission estimates for forested EVT landscapes. An adjustment was not made for the one non-forested EVT landscape due to a lack of species composition data.

2.3. Emission factors

Calculating the isoprene emission factors associated with measured emission rates removes the confounding effects of variations in canopy density and meteorological conditions in order to focus on the influence of vegetation type on isoprene emissions. Emission factors, EF, are determined as.

$$EF = \text{Emission Rate}/EAF \quad (3)$$

where EAF is the canopy average emission activity factor that accounts for the deviations expected for a given set of environmental conditions and is simply the ratio of the emission rate to the emission factor. The primary variables driving hourly to seasonal variations in isoprene emissions are LAIv, leaf temperature and PAR. Along with wind speed and humidity, which influence leaf temperature, these variables are used to calculate a canopy average EAF for each flux measurement. The resulting emission factor is representative of the average emission rate expected at standard conditions of LAIv = 5 m^2 m^{-2}, leaf surface

Fig. 1. Example of estimated half-dome flux footprint (red) for spatially averaging landcover characteristics. Each half-dome is aligned in the upwind direction with a radius of about 2 km. The distribution of high isoprene emitting trees, at 30 m spatial resolution, is shown (grey) in the background. (For interpretation of the references to color in this figure legend, the reader is referred to the web version of this article.)

temperature = 30 °C, and PAR = 1500 μmol m^{-2} s^{-1} at the top of the canopy.

EAFs were calculated using three different approaches. One approach was to calculate EAF using a single point version of the MEGANv2.1 canopy environment model for every flux measurement using the LAIv and vegetation cover developed for this study and the NLDAS-2 meteorological fields. For the second approach, EAFs were calculated using the regional MEGANv2.1 model driven by WRF derived meteorological driving variables (Guenther et al., 2012). The final approach utilized the MEGAN2.1 algorithms driven by temperature and solar radiation observed on board the aircraft in the manner described by Warneke et al. (2010).

3. Results and discussion

3.1. Airborne eddy covariance isoprene and monoterpene emission measurements

Isoprene emissions were measured by airborne wavelet-based eddy covariance for 1950 footprints (each footprint covers an area of ~6 km^2) across the southeastern US. Total monoterpene fluxes were measured for only 1284 locations. Most measurements were over forested landscapes with an average LAI of 4.85 m^2 m^{-2} and tree cover fraction of 77.3%. The average (standard deviation) isoprene emission rate was 3.61 (2.53) mg m^{-2} h^{-1} with a range of below the detection limit to 22.7 mg m^{-2} h^{-1}. Measured monoterpene emission ranged from below the detection limit to 6.57 mg m^{-2} h^{-1} with an average (standard deviation) emission rate of 0.78 (0.65) mg m^{-2} h^{-1}. Conditions were typically warm (temperature > 30 °C) and partly cloudy (PPFD <1500 μmol m^{-2} s^{-1}) resulting in an average EAF of 1.08 for isoprene and 1.28 for monoterpenes.

3.1.1. Racetrack and transect regional average measurements

Approximately 70% of the eddy covariance measurements were made during intensive stacked racetrack flight patterns where the aircraft was repeatedly flown over the same region but at different heights. The remainder of the measurements were associated with transect flights between the racetrack sites and are all grouped into one region. The 13 stacked racetrack regions and the transect flights are shown in Fig. 2 and described in Table 1. The 14 regions all had a high average tree cover percentage (66 to 94%) and LAIv (4.17 to 5.45 m^2 m^{-2}). There was a considerable difference in temperature and PAR conditions for individual regions with an isoprene EAF ranging from 0.21 to 1.46.

All of the 14 measurement regions shown in Table 1 have a significant presence of oak (*Quercus* sp.) trees (16 to 77% of tree cover and 14 to 52% of total area) which are known to be strong isoprene emitters (Rasmussen, 1970) and are referred to here as the high isoprene emitter chemotype. With the contribution of trees from six other isoprene chemotype genera (sweetgum, *Liquidambar styraciflua*; Tupelos, *Nyssa* sp.; Willows, *Salix* sp.; Locusts, *Robinia* sp., Sycamores, *Platanus* sp.; and Poplars, *Populus* sp.), the isoprene chemotype fraction in these regions ranged from 30 to 77% of total tree cover (26.8 to 54% of total landscape area). The highest fraction of isoprene emitters occurs within the Ozark mountains of Missouri and Arkansas where the isoprene chemotype is almost entirely dominated by oaks (93 to 99.6%). The measured isoprene emissions at some of these regions were relatively low (<3.5 mg m^{-2} h^{-1}) due to the cool and cloudy conditions (EAF of 0.21 to 0.38). Sweetgum contributes 16 to 41% of total isoprene emitters in six regions while Tupelo contributes 13 to 16% at two regions. Trees from the other four high isoprene chemotype genera (Willows, Locusts, Sycamores, Poplars) together contributed <6% of total isoprene emitting trees in any region. The highest average isoprene emission was recorded at Racetrack 3 which, according to the FIA species composition data, has a relatively low fraction of isoprene emitters indicating errors in the landcover data or a missing isoprene source.

Monoterpenes were not measured during all flights and data are available for only 10 of the 14 measurement regions listed in Table 1. The 12 most common tree genera comprise over 85% of the total tree cover in these regions. Guenther et al. (1994) categorized only two of these genera (Pines and Sweetgum) as high monoterpene emission chemotype. Pine trees dominate three of these regions and are codominant (with oaks) in another five regions. The remaining two regions have <10% pine tree cover. When averaged over an entire ecoregion, Pines and sweetgum together contribute from ~9% of total tree cover in oak dominated forests to about 60% in pine dominated forests. The fraction of pine and sweetgum can be higher within a specific plantation.

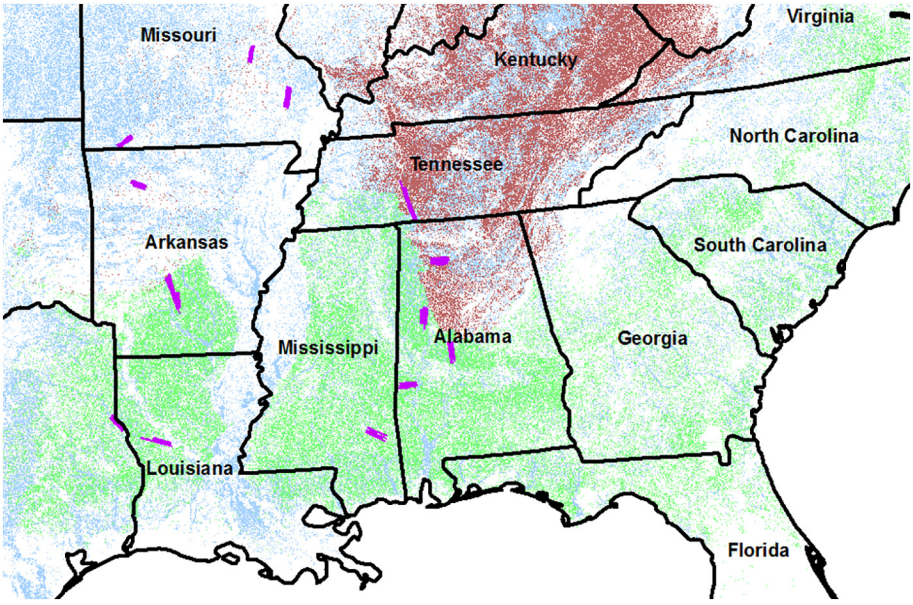

Fig. 2. Distribution of the sampled EVT classes (see Table 2) including Pine dominated forests 3194, 3349, 3371 and 3535 (light green), Oak dominated forests 3304, 3305, 3317, 3321 (dark brown) and Pine/Oak dominated landscapes 3307, 3473, 3474 and 3997 (blue). Location of racetracks intensive sampling regions are shown in purple. U.S. state boundaries (black) and names are shown for reference. (For interpretation of the references to color in this figure legend, the reader is referred to the web version of this article.)

Table 1
Racetrack and transect measurement region descriptions including leaf area index (LAI, $m^2\ m^{-2}$) and tree cover (%). Number of measurements (N), high emitter percentage of total tree cover (HEP), emission rate (ER, mg $m^{-2}\ h^{-1}$), emission activity factor (EAF, non-dimensional), emission factor (EF, mg $m^{-2}\ h^{-1}$), and emission factor of high emitting trees (EFH, mg $m^{-2}\ h^{-1}$) are shown for both isoprene and monoterpenes. A dash indicates that statistics were not calculated because the number of measurements was <20.

		Dominant	Tree		Isoprene Statistics						Total Monoterpene Statistics					
Name	Location	Trees	LAI	Cover	N	HEP	ER	EAF	EF	EFH	N	HEP	ER	EAF	EF	EFH
Transects	Various	Pine/Oak	4.76	72.3	532	32.7	3.67	1.13	4.3	13.1	375	34.1	0.65	1.27	0.59	1.72
RT 1	N. Alabama	Pine/Oak	4.99	94.3	140	43.8	3.94	0.77	6.72	15.3	80	29.1	0.87	1.22	0.86	2.95
RT 2	Texas	Pine/Oak	4.49	68.4	98	34.6	4.24	1.37	3.21	9.27	34	45.3	0.6	1.48	0.46	1.03
RT 3	Louisiana	Pine	5.21	84.7	68	26.8	7.86	1.33	7.36	27.5	0	–	–	–	–	–
RT 4	N. Missouri	Oak	5.39	67.5	29	53.9	2.53	0.21	15.4	28.6	0	–	–	–	–	–
RT 5	W. Missouri	Oak	5.3	80.0	51	49.6	2.34	0.38	8.96	18.1	0	–	–	–	–	–
RT 6	N. Arkansas	Oak	5.0	88.2	48	54.0	3.36	0.35	12.1	22.3	0	–	–	–	–	–
RT 7	S. Arkansas	Pine	5.45	80.1	239	27.0	2.59	1.0	2.94	10.9	157	59.4	0.82	1.19	0.72	1.21
RT 8	C. Alabama	Pine/Oak	4.88	81.9	99	39.7	4.47	1.15	4.61	11.6	62	29.2	0.88	1.26	0.78	2.61
RT 9	SOAS	Pine/Oak	5.11	79.6	127	31.8	3.29	1.12	3.82	12.0	107	46.9	0.68	1.19	0.61	1.3
RT 10	S. Alabama	Pine	5.41	86.4	98	28.0	3.17	1.42	2.33	8.34	93	56.1	1.02	1.48	0.72	1.28
RT 11	Mississippi	Pine	4.76	88.5	147	27.8	2.81	1.46	2.03	7.33	147	59.6	1.25	1.52	0.9	1.51
RT 12	W. Missouri	Oak	4.95	65.6	55	44.7	6.08	1.16	6.81	15.2	48	9.4	0.53	1.22	0.47	4.96
RT 13	Tennessee	Oak	4.17	72.3	123	36.3	2.95	0.85	5.64	15.5	113	8.8	0.45	1.04	0.47	5.39

3.1.2. EVT landcover class average measurements

The isoprene and monoterpene emissions associated with individual LANDFIRE EVT landcover types were estimated to investigate the utility of this high spatial resolution (30 m) scheme for characterizing BVOC emission distributions across the US. Although thirty of the EVT landcover types were dominant within the footprint of at least one airborne eddy covariance flux footprint, only the twelve EVT described in Table 2 had >20 measurements and so were included in this analysis. Sufficient ($n > 20$) monoterpene measurements were available for only eight of the EVT classes. With the exception of EVT class 3997 (pasture and hayland), the investigated EVT classes were all forests and woodlands with 68 to 96% tree cover and LAI of 3.78 to 5.29. Four of the EVTs were dominated by oak, four dominated by pines and the remainder contained both pines and oaks.

High isoprene chemotype trees comprised about one-third to two-thirds of total tree cover in the twelve EVTs classes. The average isoprene emission rate measured for the EVTs ranged over about a factor of 5 from 1.89 to 9.78 mg $m^{-2}\ h^{-1}$. The highest average isoprene emission rates (>8.6 mg $m^{-2}\ h^{-1}$) were observed over forests comprised predominately of oaks. A lack of monoterpene emission measurements for two EVTs reduced the number characterized to ten. The contribution of high monoterpene chemotype trees to total tree cover when averaged over EVT ecoregions ranged from about 6 to 60%.

3.2. Comparison of airborne direct and indirect isoprene emission estimates

Isoprene flux data derived from the airborne wavelet-based eddy covariance direct flux measurement approach were compared with the airborne mass balance indirect flux measurement method described by Warneke et al. (2010). The mean emission factor for all measurements determined with the indirect inverse model approach (6.1 mg $m^{-2}\ h^{-1}$) is about 30% higher than the mean value (4.7 mg $m^{-2}\ h^{-1}$) based on the eddy covariance approach. However, it should be noted that the footprints of these two measurement techniques differ considerably, including a larger footprint size for the mass balance approach, and so the estimates for individual measurements are not expected to agree perfectly since they represent somewhat different landscapes. The means of the direct and indirect isoprene emission factor estimates for the racetrack regional averages are within 7% and the means of the EVT landcover average values are within 13% indicating that the regional averages from the two techniques are in good agreement. Fig. 3 shows that the EVT average values and the racetrack average values for the two approaches follow the same pattern, with both approaches having higher values for oak dominated forests and lower values for pine woods, but there is considerable variability in different regions which may be at least partly due to the differences in the footprints associated with the two techniques. A semivariogram analysis (Garrigues et al., 2006) of the distribution of isoprene emitters, based on LANDFIRE landcover data, indicates that the region with the largest difference, more than a factor of 3, between the indirect and direct approaches had a substantially higher spatial variability on a scale of 1 to 5 km. The variabilities become similar when the distance increases to approximately 10 km, the same order as the footprint size of the inverse model flux measurement. This may explain why there is overall agreement even though there are considerable differences at smaller scales including individual flight segments.

Table 2
LANDFIRE Existing Vegetation Type (EVT) descriptions including leaf area index (LAI, $m^2\ m^{-2}$) and tree cover (%). Number of measurements (N), high emitter percentage of total tree cover (HEP), emission activity factor (EAF, non-dimensional), emission factor (EF, mg $m^{-2}\ h^{-1}$), and emission factor of high emitting trees (EFH, mg $m^{-2}\ h^{-1}$) are shown for both isoprene and monoterpenes. A dash indicates that statistics were not calculated because the number of measurements was <20.

EVT		Dominant	% Tree		Isoprene Statistics						Total Monoterpene Statistics					
ID	Description	Trees	LAI	Cover	N	HEP	EAF	EF	EFH		N	HEP	ER	EAF	EF	EFH
3194	Ruderal upland- treed	Pine	4.98	81.0	247	38.1	1.15	3.90	12.6		187	53.7	0.76	1.25	0.66	1.23
3304	Ozark-Ouachita Oaks	Oak	5.13	75.8	261	62.9	0.59	9.78	20.5		71	14.6	0.46	1.20	0.42	2.87
3305	Interior Plateau Oaks	Oak	4.21	68.3	193	42.4	0.90	5.43	18.8		111	11.8	0.46	1.07	0.48	4.07
3307	Gulf Upland hardwoods	Pine/Oak	3.78	68.4	23	46.5	0.81	7.48	23.5		24	36.6	0.56	1.01	0.6	1.64
3317	Allegheny Oaks	Oak	4.94	93.5	65	41.1	0.66	8.64	22.5		25	14.1	1.10	1.19	1.16	8.21
3321	Southcentral forest	Oak	5.11	95.7	69	35.9	0.90	5.27	15.3		54	6.2	0.76	1.26	0.7	11.3
3349	E. Gulf Pine woods	Pine	4.64	88.8	115	30.1	1.45	1.89	7.1		116	59.5	1.34	1.50	0.98	1.65
3371	W. Gulf Pine forest	Pine	5.29	81.5	43	28.7	1.32	3.50	14.9		18	–	–	–	–	–
3473	Gulf Floodplain	Pine/Oak	5.17	79.5	131	47.5	1.29	5.62	14.9		71	34.1	0.86	1.42	0.66	1.94
3474	Gulf Riparian woods	Pine/Oak	4.95	84.3	23	40.7	1.34	3.89	11.3		14	–	–	–	–	–
3535	Southeast tree plantations	Pine	5.17	78.9	600	31.9	1.23	3.22	12.8		445	59.7	0.84	1.35	0.67	1.12
3997	Pasture and Hayland	Pine/Oak	3.23	48.9	84	39.2	1.24	3.05	15.9		64	51.0	0.62	1.13	0.63	1.23

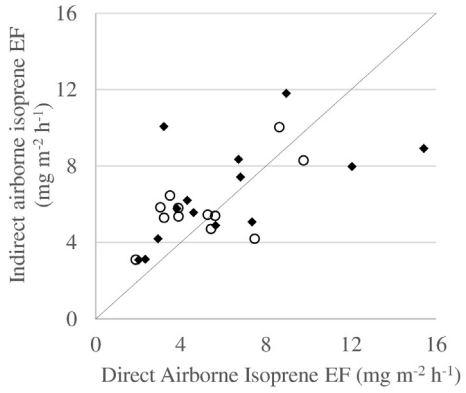

Fig. 3. Comparison of isoprene emission factors averaged over individual EVT landcover types (solid diamonds) and racetrack regions (open circles) using direct airborne eddy covariance and indirect inverse model airborne mass balance flux approaches. The dashed line indicates a slope of 1:1.

3.3. Isoprene emission factors

Geron et al. (2001) used enclosure measurements with light and temperature control to quantify isoprene emission rates from all seven of the major U.S. isoprene emitting broadleaf tree genera (Oaks, Sweetgum, Tupelos, Willows, Locusts, Sycamores and Poplars). They found that the isoprene emission rate variability among these seven genera of U.S. isoprene emitting broadleaf trees was similar to the level of variability within a genus or even a species or an individual tree. This finding simplifies efforts in this region to relate airborne isoprene flux measurements to isoprene emission factors comparable with leaf level measurements by defining just two tree isoprene emission chemotypes (emitters and non-emitters). Note that there are other U.S. trees, such as palms and the needleleaf spruce (*Picea* sp.), that have a different isoprene chemotype, with substantially lower but non-negligible isoprene emission rates. Also, it is notable that there are some members of these seven genera, native to regions outside of the U.S., that are non-emitters, such as *Quercus ilex*, but they are not a significant part of the landscapes in the southeastern U.S.

The average of the landscape-averaged EF determined from airborne eddy covariance measurements was 4.73 with a range of 2.03 to 15.4 mg m^{-2} h^{-1} for individual regions. Since isoprene emitting trees cover an average of 36.4% of the surface area, based on the MEGAN2.1 landcover data, the isoprene emission factor of the isoprene emitting trees is estimated to be 13 mg m^{-2} h^{-1} which is about half of the MEGAN2.1 EF (24 mg m^{-2} h^{-1}) assigned to these isoprene emitting trees. Fig. 4 shows that the landscape average EF has a range of about a factor of 4. The EF increase is associated with an increase in the fraction of isoprene emitting tree cover but the factor of 4 increase in EF is associated with an isoprene tree cover increase of only a factor of two. This is contrary to the expectation that the contribution of non-tree isoprene emitters should be higher in landscapes with a lower tree fraction and so there should be an emission increase of slightly less than a factor of two associated with a factor of two increase in isoprene emitting tree cover. Fig. 4 illustrates the relationship between isoprene EF of isoprene emitting trees and the fraction of the landscape covered by isoprene emitting trees. The estimated contribution of non-tree isoprene emission is about 2 to 15% of total isoprene emission in these regions. The regions with an isoprene emitting canopy cover fraction of <50% have an EF of 12 ± 3 mg m^{-2} h^{-1} with the exception of the region in Louisiana which had a much higher EF. If we consider only the regions where isoprene emitting trees cover more than half of the area then the average EF is about 23 mg m^{-2} h^{-1}. This is in remarkably good agreement with the value of 24 mg m^{-2} h^{-1} assigned to these isoprene emitting trees in the MEGAN2.1 model.

Bryan et al. (2015) used a 1D model to investigate the impact of canopy heterogeneity on whole canopy isoprene emissions in a northern Michigan forest and found that accounting for the vertical profile of the fraction of isoprene emitting trees modified the estimated emissions by 34%. The canopy at that site had a higher fraction of isoprene emitters (oaks and poplars) in the upper canopy which led to higher isoprene emissions due to the increased availability of sunlight. In contrast, isoprene emitters tend to be in the understory in pine plantations in the southeastern US leading to lower emissions than expected for the canopy average isoprene emitting fraction (Stroud et al., 2005). This may explain the strong increase in the canopy average isoprene EF for isoprene emitting trees, shown in Fig. 4, from landscapes with a low fraction of isoprene emitters, such as pine plantations with oak and

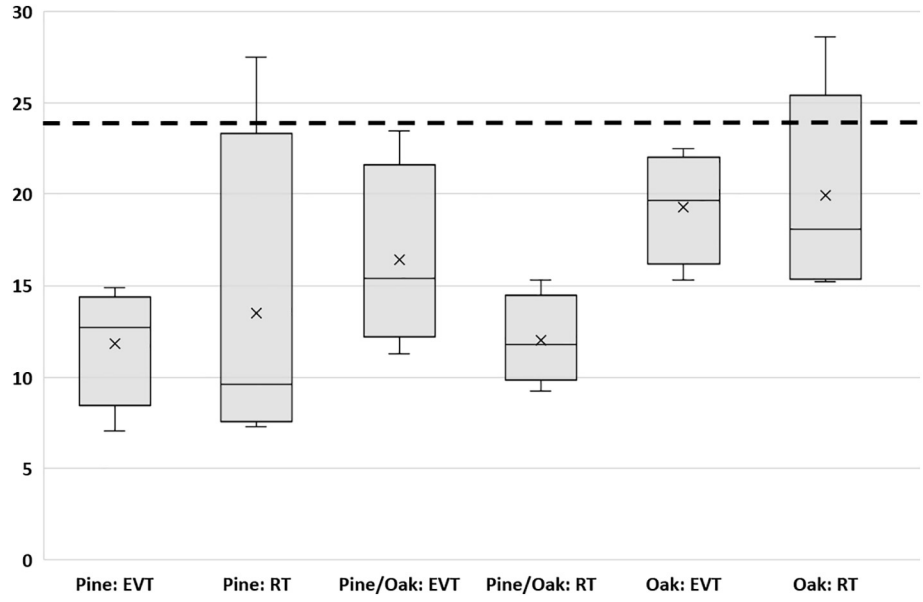

Fig. 4. Isoprene emission factors determined for oaks and other high isoprene emitting trees (isoprene EFH in Tables 1 and 2) using aircraft eddy covariance averaged over racetracks (RT) and Existing Vegetation Type (EVT) landscapes dominated by either pine trees, oak trees, or similar amounts of oak and pine. The boxes indicate the first to third quartile. The bottom, middle and top line indicate the minimum, median and maximum values and the X indicates the mean value. The dashed line shows the value used in MEGANv2.1.

sweetgum understory, to landscapes with a high fraction of isoprene emitters.

3.4. Monoterpene emission factors

Unlike isoprene emitters, which can often be considered to be either non-emitters or high-emitters in the southeastern US, monoterpene emissions are more widespread with many trees, shrubs and herbs capable of at least some level of monoterpene production and emission (Guenther, 2013). Guenther et al. (1994) classified U.S. tree species into 5 monoterpene emission chemotypes, with total monoterpene emission rates that vary over a factor of 30. Of the 85 tree genera contained in the US FIA version 1.0 database (Miles et al., 2001), MEGAN2.1 classifies 11 as high MT emitters, 12 as moderate emitter, 22 as low emitters, 17 as very low emitters, and 23 as negligible emitters.

The average of the landscape average (standard deviation) total monoterpene emission factor for all measurements was 0.66 (0.59) mg m^{-2} h^{-1}. Values were somewhat higher (0.66 to 0.98 mg m^{-2} h^{-1}) in landscapes dominated by pine trees and tended to be lower in landscapes dominated by oaks (0.47 to 0.7 mg m^{-2} h^{-1}) with the exception of the Allegheny Oak EVT which had the highest landscape average EF (1.16 mg m^{-2} h^{-1}) of any EVT. About 38% of the trees in the studied regions were high monoterpene chemotypes and they covered about 30% of the landscape. If high monoterpene chemotype trees were responsible for all of the observed monoterpene emissions then the resulting monoterpene emission factor would be 2.2 mg m^{-2} h^{-1} which is 33% higher than the value (1.65 mg m^{-2} h^{-1}) used for MEGAN2.1. Fig. 5 shows that the monoterpene emission factor determined for regions where 35% or more of the landscape is covered by high monoterpene chemotype trees is about 20% lower than the MEGAN2.1 emission factor. The observed monoterpene emission factor is much higher when these trees are a small fraction of the landscape which indicates that unaccounted processes, such as floral emissions or light dependent emissions, or sources such as non-tree vegetation and moderate or low monoterpene chemotype trees are likely making the dominant contribution to the total landscape monoterpene emission.

3.5. Assessment of uncertainties

LAIv distributions estimated for different years and with different processing approaches have the same general patterns but there are significant deviations that could influence estimation of BVOC EFs. Relatively high and constant LAIv occurs over much of the southeastern US, associated with dense forest cover and small seasonal variations. The considerable interannual variability in LAIv (1 to 2 m^2 m^{-2}) indicates that using climatological LAIv values, instead of the time specific values used for this study, could result in errors of about 15% for isoprene and 20% or more for monoterpenes. Isoprene emissions are less sensitive because emissions become saturated at higher LAI due to limited light availability.

The PFT database developed for this project has tree PFT distributions that are relatively similar to the MEGAN PFT data (PFT data version 2.2), which is expected since both were calculated using FIA tree ground survey data and the satellite-based tree cover data. The main difference is that the data were averaged over different landcover type zones: the new PFT data uses the more highly resolved LANDFIRE EVT data in comparison to the ecoregion scheme used for the MEGAN2.2 PFT data. In contrast, the shrub and grass distributions are considerably different in both spatial distributions and vegetation cover percentages and crop distributions have different cover percentages. This is because these ground cover types are less constrained by ground survey observations. However, the total ground cover (non-tree) is constrained by satellite observations and is similar in the two databases. Since trees tend to have much higher isoprene emission rates (Rasmussen, 1970), models estimate that non-tree vegetation makes only a small contribution to the total isoprene emission in the regions studied here and is expected to have little impact on these results.

There are considerable differences in EF results when they are calculated using EAF based on WRF instead of NLDAS-2 meteorological data. The WRF based EF values were consistently lower (~37%) due to higher EAF values based on the higher WRF solar radiation and temperature. Solar radiation and temperature biases in WRF simulations have previously been reported to result in isoprene EAF overestimates of 23 to 37% (Wang et al., 2011; Carlton and Baker, 2011; Guenther et al., 2012) and have been associated with underestimates of light scattering by clouds and haze. This demonstrates the importance of accurate meteorological

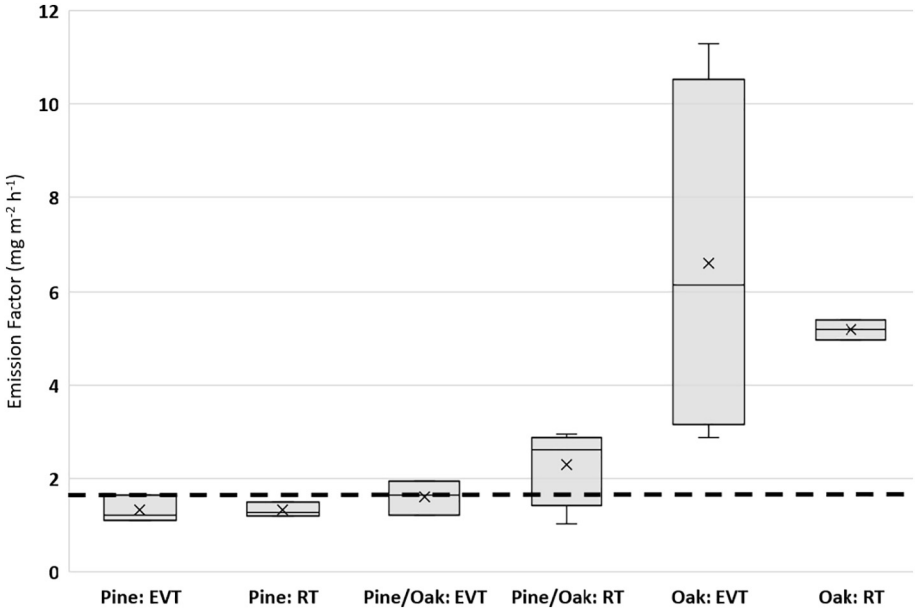

Fig. 5. Monoterpene emission factors determined for pines and other high monoterpene emitting trees (monoterpene EFH in Tables 1 and 2) using aircraft eddy covariance averaged over racetracks (RT) and Existing Vegetation Type (EVT) landscapes (see Tables 1 and 2) dominated by either pine trees, oak trees, or similar amounts of oak and pine. The boxes indicate the first to third quartile. The bottom, middle and top line indicate the minimum, median and maximum values and the X indicates the mean value. The dashed line shows the value used in MEGANv2.1.

observations for determine both EFs from airborne emission measurements and for biogenic VOC emission modeling. Since the NLDAS-2 data includes assimilation of observed meteorology, we expect it to be more accurate than WRF model simulations without data assimilation but recognize that there are still substantial uncertainties.

The landcover data used for biogenic emission modeling are developed by extrapolating plant species composition data from ground measurements with satellite based landcover distribution maps. The LANDFIRE EVT data has a large number (635) of vegetation types and a high spatial resolution (30 m) and so is expected to be more suitable for biogenic VOC emission modeling than previous datasets. However, it should be noted that a high spatial resolution creates greater uncertainties associated with matching airborne emission measurements with landcover in a specific footprint. A comparison of fluxes averaged over 2-km, 4-km and 6-km footprints showed that calculated fluxes varied by <15% indicating a relatively small impact of footprint spatial resolution on the magnitude of airborne EF estimates and indicating that 2-km is a reasonable scale for calculating airborne fluxes and comparing with 30-m resolution landcover types.

4. Conclusions

Isoprene and monoterpene emissions from the major forest types in the southeastern US, primarily oak and pine dominated forests, were directly measured using the airborne wavelet-based eddy covariance measurement technique. The measurements were compared with an independent approach that was previously used to estimate fluxes from airborne observations (Warneke et al., 2010) and the two methods agreed within about 10% when the means of the regional averages were compared. The differences were greater when estimates for individual locations were compared, especially in regions of high emission variability, which is likely due to the difference in the flux footprints for the two measurement approaches.

Emission models must account for both the temporal variability, driven primarily by emission response to solar radiation and temperature, and the spatial variability driven primarily by distributions of chemotype compositions. Long-term measurements with tower-based eddy covariance flux systems have provided a means to evaluate and improve algorithms simulating temporal variations (e.g., Rantala et al., 2015; Seco et al., 2015). Airborne measurement systems provide a complementary approach for characterizing spatial variability across large regions. Misztal et al. (2014) demonstrated this in a relatively less complex landscape in that a single genus, oak, is the dominant source of isoprene. For this study we investigated a region that has a larger contribution from other isoprene emitting genera but is still dominated by oaks and there is evidence that all of these isoprene emitting trees in this region have a similar emission capacity and can be considered to be a single chemotype. The isoprene emission factor for oaks and other high emitters estimated from airborne eddy covariance measurements over oak dominated forests agree well (within 20%) with the value used in the MEGAN2.1 model. The aircraft measurement based emission factor associated with high emitters in landscapes dominated by pines and other non- isoprene emitters is 50% lower. This may be an indication that measurements of isoprene emissions from oaks and other higher emitters cannot reliably be determined from pine forests and other landscapes with a low abundance of these plants. Another possible explanation is the tendency of isoprene emitters to be present in the understory of pine dominated canopies where isoprene emission is suppressed by a lack of sunlight. This finding emphasizes the need to investigate the importance of canopy vertical heterogeneity of isoprene emitting fraction in biogenic emission models.

Relating aircraft measurements of total monoterpene emissions to individual vegetation types is more complicated due to the larger diversity of monoterpene chemotypes. However, using the MEGAN2.1 categorization of monoterpene chemotypes, the emission factor estimated from airborne fluxes measurements is similar (20% lower) to the MEGAN2.1 value. The emission factor is much higher (more than a factor of 3) for oak forests with a small fraction of high monoterpene emitters which may indicate the that the monoterpene emission from pine and other high monoterpene emitting plants cannot be reliably determined from measurements over oak forests and similar landscapes. It may also indicate a need to account for other monoterpene emission processes, such as stress or floral or light dependent emissions, or emissions from other vegetation types.

Author contributions

A. Guenther, T. Karl, C. Warneke, M. Graus, A. Goldstein, L. Kaser, and P. Misztal planned and organized the project. L. Kaser, B. Yuan, T. Karl, C. Warneke and M. Graus conducted measurements of isoprene and monoterpenes by PTR-MS. H. Yu, A. Guenther, L. Kaser, T. Karl, D. Gu, and C. Warneke analyzed airborne measurement data. H. Yu, A. Guenther and C. Geron analyzed model results. A. Guenther and H. Yu wrote the manuscript. All authors reviewed and commented on the paper.

Competing financial interests

The authors declare that they have no conflict of interest.

Acknowledgements

Haofei Yu, Dasa Gu, Carsten Warneke and Alex Guenther were partially supported by the State of Texas through the Air Quality Research Program administered by The University of Texas at Austin by means of Grant 14-016 from the Texas Commission on Environmental Quality and Alex Guenther was partially supported by National Aeronautics and Space Administration (NASA) Atmospheric Composition Campaign Data Analysis and Modeling (ACCDAM) program award NNX15AT62G. Allen Goldstein and Pawel Misztal were supported by United States Environmental Protection Agency Grant Number R835407. Thomas Karl was supported by the European Commission Seventh Framework Programme (Marie Curie Reintegration Program, “ALP-AIR”, grant no. 334084). We thank Greg Yarwood and Sue Kemball-Cook of Ramboll Environ and Mark Estes and Doug Boyer of the Texas Commission on Environmental Quality for their valuable advice and comments on this project and for supplying WRF model output.

References

Brown, S.S., deGouw, J.A., Warneke, C., Ryerson, T.B., Dubé, W.P., Atlas, E., Weber, R.J., Peltier, R.E., Neuman, J.A., Roberts, J.M., Swanson, A., Flocke, F., McKeen, S.A., Brioude, J., Sommariva, R., Trainer, M., Fehsenfeld, F.C., Ravishankara, A.R., 2009. Nocturnal isoprene oxidation over the Northeast United States in summer and its impact on reactive nitrogen partitioning and secondary organic aerosol. Atmos. Chem. Phys. 9:3027–3042. http://dx.doi.org/10.5194/acp-9-3027-2009.

Broxton, P.D., Zeng, X., Scheftic, W., Troch, P.A., 2014. A MODIS-based global 1-km maximum green vegetation fraction dataset. J. Appl. Meteorol. Climatol. 53:1996–2004. http://dx.doi.org/10.1175/JAMC-D-13-0356.1.

Bryan, A.M., Cheng, S.J., Ashworth, K., Guenther, A.B., Hardiman, B.S., Bohrer, G., Steiner, A.L., 2015. Forest-atmosphere BVOC exchange in diverse and structurally complex canopies: 1-D modeling of a mid-successional forest in northern Michigan. Atmos. Environ. 120, 217–226.

Carlton, A.G., Baker, K.R., 2011. Photochemical modeling of the Ozark Isoprene Volcano: MEGAN, BEIS, and their impacts on air quality predictions. Environ. Sci. Technol. 45:4438–4445. http://dx.doi.org/10.1021/es200050x.

Carlton, A.G., Wiedinmyer, C., Kroll, J.H., 2009. A review of secondary organic aerosol (SOA) formation from isoprene. Atmos. Chem. Phys. 9:4987–5005. http://dx.doi.org/10.5194/acp-9-4987-2009.

Chameides, W.L., Lindsay, R.W., Richardson, J., Kiang, C.S., 1988. The role of biogenic hydrocarbons in urban photochemical urban photochemical smog – Atlanta as a case-study. Science 241, 1473–1475.

Fang, H., Jiang, C., Li, W., Wei, S., Baret, F., Chen, J.M., Garcia-Haro, J., Liang, S., Liu, R., Myneni, R.B., Pinty, B., Xiao, Z., Zhu, Z., 2013. Characterization and intercomparison of global moderate resolution leaf area index (LAI) products: analysis of climatologies and theoretical uncertainties. J. Geophys. Res. Biogeosci. 118:529–548. http://dx.doi.org/10.1002/jgrg.20051.

Garrigues, S., Allard, D., Baret, F., Weiss, M., 2006. Quantifying spatial heterogeneity at the landscape scale using variogram models. Remote Sens. Environ. 103, 81–96.

Geron, C., Harley, P., Guenther, A., 2001. Isoprene emission capacity for US tree species. Atmos. Environ. 35, 3341–3352.

Goldstein, A.H., Galbally, I.E., 2007. Known and unexplored organic constituents in the Earth's atmosphere. Environ. Sci. Technol. 41:1514–1521. http://dx.doi.org/10.1021/es072476p.
Greenberg, J.P., Guenther, A., Zimmerman, P., Baugh, W., Geron, C., Davis, K., Helmig, D., Klinger, L.F., 1999. Tethered balloon measurements of biogenic VOCs in the atmospheric boundary layer. Atmos. Environ. 33 (6), 855–867.
Guenther, A., 2013. Biological and chemical diversity of biogenic volatile organic emissions into the atmosphere. Atmos. Sci. 2013:27. http://dx.doi.org/10.1155/2013/786290.
Guenther, A., Zimmerman, P., Wildermuth, M., 1994. Natural Volatile Organic-Compound Emission Rate Estimates for United-States Woodland Landscapes. Atmos. Environ. 28, 1197–1210.
Guenther, A., Hewitt, C.N., Erickson, D., Fall, R., Geron, C., Graedel, T., Harley, P., Klinger, L., Lerdau, M., McKay, W.A., Pierce, T., Scholes, B., Steinbrecher, R., Tallamraju, R., Taylor, J., Zimmerman, P., 1995. A global model of natural volatile organic compound emissions. J. Geophys. Res. Atmos. 100:8873–8892. http://dx.doi.org/10.1029/94JD02950.
Guenther, A., Baugh, W., Davis, K., Hampton, G., Harley, P., Klinger, L., Vierling, L., Zirmnennan, P., Allwine, E., Dilts, S., 1996. Isoprene fluxes measured by enclosure, relaxed eddy accumulation, surface layer gradient, mixed layer gradient, and mixed layer mass balance techniques. J. Geophys. Res. 101 (18), 555–518,567.
Guenther, A., Karl, T., Harley, P., Wiedinmyer, C., Palmer, P., Geron, C., 2006. Estimates of global terrestrial isoprene emissions using MEGAN (Model of Emissions of Gases and Aerosols from Nature). Atmos. Chem. Phys. 6, 3181–3210.
Guenther, A., Jiang, X., Heald, C., Sakulyanontvittaya, T., Duhl, T., Emmons, L., Wang, X., 2012. The Model of Emissions of Gases and Aerosols from Nature version 2.1 (MEGAN2. 1): an extended and updated framework for modeling biogenic emissions. Geosci. Model Dev. 5 (6), 1471–1492.
Guo, H., Ling, Z., Simpson, I., Blake, D., Wang, D., 2012. Observations of isoprene, methacrolein (MAC) and methyl vinyl ketone (MVK) at a mountain site in Hong Kong. J. Geophys. Res. Atmos. 117 (1984–2012).
Hu, Y., Chang, M.E., Russell, A.G., Odman, M.T., 2010. Using synoptic classification to evaluate an operational air quality forecasting system in Atlanta. Atmospheric Pollution Research 1: 280–287. http://dx.doi.org/10.5094/APR.2010.035.
Karl, T., Apel, E., Hodzic, A., Riemer, D., Blake, D., Wiedinmyer, C., 2009. Emissions of volatile organic compounds inferred from airborne flux measurements over a megacity. Atmos. Chem. Phys. 9, 271–285.
Karl, T., Misztal, P., Jonsson, H., Shertz, S., Goldstein, A., Guenther, A., 2013. Airborne flux measurements of BVOCs above Californian oak forests: experimental investigation of surface and entrainment fluxes, OH densities, and Damköhler numbers. J. Atmos. Sci. 70, 3277–3287.
Kaser, L., Karl, T., Yuan, B., Mauldin, R.L., Cantrell, C.A., Guenther, A.B., Patton, E.G., Weinheimer, A.J., Knote, C., Orlando, J., Emmons, L., Apel, E., Hornbrook, R., Shertz, S., Ullmann, K., Hall, S., Graus, M., de Gouw, J., Zhou, X., Ye, C., 2015. Chemistry-turbulence interactions and mesoscale variability influence the cleansing efficiency of the atmosphere. Geophys. Res. Lett. 42 (24), 10,894–810,903.
Kesselmeier, J., Staudt, M., 1999. Biogenic volatile organic compounds (VOC): an overview on emission, physiology and ecology. J. Atmos. Chem. 33 (1), 23–88.
Kota, S.H., Schade, G., Estes, M., Boyer, D., Ying, Q., 2015. Evaluation of MEGAN predicted biogenic isoprene emissions at urban locations in Southeast Texas. Atmos. Environ. 110:54–64. http://dx.doi.org/10.1016/j.atmosenv.2015.03.027.
Lamarque, J.F., Bond, T.C., Eyring, V., Granier, C., Heil, A., Klimont, Z., Lee, D., Liousse, C., Mieville, A., Owen, B., Schultz, M.G., Shindell, D., Smith, S.J., Stehfest, E., Van Aardenne, J., Cooper, O.R., Kainuma, M., Mahowald, N., McConnell, J.R., Naik, V., Riahi, K., van Vuuren, D.P., 2010. Historical (1850–2000) gridded anthropogenic and biomass burning emissions of reactive gases and aerosols: methodology and application. Atmos. Chem. Phys. 10:7017–7039. http://dx.doi.org/10.5194/acp-10-7017-2010.
Lenschow, D., Mann, J., Kristensen, L., 1994. How long is long enough when measuring fluxes and other turbulence statistics? J. Atmos. Ocean. Technol. 11, 661–673.
Mauder, M., Desjardins, R.L., MacPherson, I., 2007. Scale analysis of airborne flux measurements over heterogeneous terrain in a boreal ecosystem. J. Geophys. Res. Atmos. 112 (1984–2012).
Miles, P., Brand, G., Alerich, C., Bednar, L., Woudenberg, S., Glover, J., Ezzell, E., 2001. The Forest Inventory and Analysis Database: Database Description and Users Manual Version 1.0, USDA Forest Service North Central Research Station, General Technical Report NC – 218, St. Paul, MN USA.
Misztal, P., Karl, T., Weber, R., Jonsson, H., Guenther, A.B., Goldstein, A.H., 2014. Airborne flux measurements of biogenic isoprene over California. Atmos. Chem. Phys. 14, 10631–10647.
Misztal, P.K., Avise, J.C., Karl, T., Scott, K., Jonsson, H.H., Guenther, A.B., Goldstein, A.H., 2016. Evaluation of regional isoprene emission factors and modeled fluxes in California. Atmos. Chem. Phys. 16:9611–9628. http://dx.doi.org/10.5194/acp-16-9611-2016.
Odman, M.T., Hu, Y., Russell, A.G., Chang, M.E., 2007. Forecasting ozone and $PM_{2.5}$ in southeastern US. In: Borrego, C., Renner, E. (Eds.), Air Pollution Modeling and its Application XVIII. Elsevier, Amsterdam, The Netherlands, pp. 220–229.
Oleson, K.W., Lawrence, D.M., Bonan, G.B., Drewniak, B., Huang, M., Koven, C.D., Levis, S., Li, F., Riley, W.J., Subin, Z.M., Swenson, S.C., Thornton, P.E., Bozbiyik, A., Fisher, R., Heald, C.L., Kluzek, E., Lamarque, J.-F., Lawrence, P.J., Leung, L.R., Lipscomb, W., Muszala, S., Ricciuto, D.M., Sacks, W., Sun, Y., Tang, J., Yang, Z.-L., 2013. Technical Description of Version 4.5 of the Community Land Model (CLM). National Center for Atmospheric Research, Boulder, Colorado. U.S.A.
Omernik, J.M., Griffith, G.E., 2004. Ecoregions of the conterminous United States: evolution of a hierarchical spatial framework. Environ. Manag. 54 (6), 1249–1266.
Pachauri, R.K., Allen, M., Barros, V., Broome, J., Cramer, W., Christ, R., Church, J., Clarke, L., Dahe, Q., Dasgupta, P., 2014. Climate Change 2014: Synthesis Report. Contribution of Working Groups I, II and III to the Fifth Assessment Report of the Intergovernmental Panel on Climate Change.
Rantala, P., Aalto, J., Taipale, R., Ruuskanen, T.M., Rinne, J., 2015. Annual cycle of volatile organic compound exchange between a boreal pine forest and the atmosphere. Biogeosciences 12: 5753–5770. http://dx.doi.org/10.5194/bg-12-5753-2015.
Rasmussen, R.A., 1970. Isoprene: identified as a forest-type emission to the atmosphere. Environ. Sci. Technol. 4, 667–671.
Ryan, K.C., Opperman, T.S., 2013. LANDFIRE – a national vegetation/fuels data base for use in fuels treatment, restoration, and suppression planning. For. Ecol. Manag. 294, 208–216.
Seco, R., Karl, T., Guenther, A., Hosman, K.P., Pallardy, S.G., Gu, L., Geron, C., Harley, P., Kim, S., 2015. Ecosystem-scale volatile organic compound fluxes during an extreme drought in a broadleaf temperate forest of the Missouri Ozarks (central USA). Glob. Chang. Biol. 21 (10), 3657–3674.
Stroud, C., Makar, P., Karl, T., Guenther, A., Geron, C., Turnipseed, A., Nemitz, E., Baker, B., Potosnak, M., Fuentes, J.D., 2005. Role of canopy-scale photochemistry in modifying biogenic-atmosphere exchange of reactive terpene species: Results from the CELTIC field study. J. Geophys. Res.-Atmos. 110 (D17).
U.S. Environmental Protection Agency, 2014. Health Risk and Exposure Assessment for Ozone. Final Report, U.S. Environmental Protection Agency, Research Triangle Park, North Carolina. 27711.
Wang, X.M., Situ, S.P., Guenther, A., Chen, F., Wu, Z.Y., Xia, B.C., Wang, T.J., 2011. Spatiotemporal variability of biogenic terpenoid emissions in Pearl River Delta, China, with high-resolution land-cover and meteorological data. Tellus Ser. B Chem. Phys. Meteorol. 63:241–254. http://dx.doi.org/10.1111/j.1600-0889.2010.00523.x.
Warneke, C., de Gouw, J.A., Del Negro, L., Brioude, J., McKeen, S., Stark, H., Kuster, W.C., Goldan, P.D., Trainer, M., Fehsenfeld, F.C., Wiedinmyer, C., Guenther, A.B., Hansel, A., Wisthaler, A., Atlas, E., Holloway, J.S., Ryerson, T.B., Peischl, J., Huey, L.G., Hanks, A.T.C., 2010. Biogenic emission measurement and inventories determination of biogenic emissions in the eastern United States and Texas and comparison with biogenic emission inventories. J. Geophys. Res. Atmos. 115. http://dx.doi.org/10.1029/2009JD012445 (n/a-n/a).
Warneke, C., Trainer, M., de Gouw, J.A., Parrish, D.D., Fahey, D.W., Ravishankara, A.R., Middlebrook, A.M., Brock, C.A., Roberts, J.M., Brown, S.S., Neuman, J.A., Lerner, B.M., Lack, D., Law, D., Hübler, G., Pollack, I., Sjostedt, S., Ryerson, T.B., Gilman, J.B., Liao, J., Holloway, J., Peischl, J., Nowak, J.B., Aikin, K.C., Min, K.E., Washenfelder, R.A., Graus, M.G., Richardson, M., Markovic, M.Z., Wagner, N.L., Welti, A., Veres, P.R., Edwards, P., Schwarz, J.P., Gordon, T., Dube, W.P., McKeen, S.A., Brioude, J., Ahmadov, R., Bougiatioti, A., Lin, J.J., Nenes, A., Wolfe, G.M., Hanisco, T.F., Lee, B.H., Lopez-Hilfiker, F.D., Thornton, J.A., Keutsch, F.N., Kaiser, J., Mao, J., Hatch, C.D., 2016. Instrumentation and measurement strategy for the NOAA SENEX aircraft campaign as part of the Southeast Atmosphere Study 2013. Atmos. Meas. Tech. 9:3063–3093. http://dx.doi.org/10.5194/amt-9-3063-2016.
Xia, Y., Mitchell, K., Ek, M., Sheffield, J., Cosgrove, B., Wood, E., Luo, L., Alonge, C., Wei, H., Meng, J., Livneh, B., Lettenmaier, D., Koren, V., Duan, Q., Mo, K., Fan, Y., Mocko, D., 2012. Continental-scale water and energy flux analysis and validation for the North American Land Data Assimilation System project phase 2 (NLDAS-2): 1. Intercomparison and application of model products. J. Geophys. Res. Atmos. 117. http://dx.doi.org/10.1029/2011JD016048 (n/a-n/a).
Yuan, B., Kaser, L., Karl, T., Graus, M., Peischl, J., Campos, T.L., Shertz, S., Apel, E.C., Hornbrook, R.S., Hills, A., Gilman, J.B., Lerner, B.M., Warneke, C., Flocke, F.M., Ryerson, T.B., Guenther, A.B., de Gouw, J.A., 2015. Airborne flux measurements of methane and volatile organic compounds over the Haynesville and Marcellus shale gas production regions. J. Geophys. Res. Atmos. 120, 6271–6289.
Zare, A., Christensen, J.H., Irannejad, P., Brandt, J., 2012. Evaluation of two isoprene emission models for use in a long-range air pollution model. Atmos. Chem. Phys. 12:7399–7412. http://dx.doi.org/10.5194/acp-12-7399-2012.
Zhang, R., Suh, I., Lei, W., Clinkenbeard, A.D., North, S.W., 2000. Kinetic studies of OH-initiated reactions of isoprene. J. Geophys. Res. Atmos. 105:24627–24635. http://dx.doi.org/10.1029/2000JD900330.
Zimmerman, P.R., Greenberg, J.P., Westberg, C.E., 1988. Measurements of atmospheric hydrocarbons and biogenic emission fluxes in the Amazon boundary-layer. J. Geophys. Res.-Atmos. 93 (D2), 1407–1416.